TECHNICAL REPORTS

nature medicine

On silico peptide microarrays for high-resolution mapping of antibody epitopes and diverse protein-protein interactions

Jordan V Price[1], Stephanie Tangsombatvisit[1], Guangyu Xu[2], Jiangtao Yu[2], Dan Levy[3], Emily C Baechler[4], Or Gozani[3], Madoo Varma[2,5], Paul J Utz[1,5] & Chih Long Liu[1,5]

We developed a new, silicon-based peptide array for a broad range of biological applications, including potential development as a real-time point-of-care platform. We used photolithography on silicon wafers to synthesize microarrays (Intel arrays) that contained every possible overlapping peptide within a linear protein sequence covering the N-terminal tail of human histone H2B. These arrays also included peptides with acetylated and methylated lysine residues, reflecting post-translational modifications of H2B. We defined minimum binding epitopes for commercial antibodies recognizing the modified and unmodified H2B peptides. We further found that this platform is suitable for the highly sensitive characterization of methyltransferases and kinase substrates. The Intel arrays also revealed specific H2B epitopes that are recognized by autoantibodies in individuals with systemic lupus erythematosus who have elevated disease severity. By combining emerging nonfluorescence-based detection methods with an underlying integrated circuit, we are now poised to create a truly transformative proteomics platform with applications in bioscience, drug development and clinical diagnostics.

The development of highly multiplex, inexpensive proteomics tools is crucial to deliver on the promise of individualized medicine and point-of-care diagnosis[1]. We previously described a diverse group of array technologies to profile autoantibodies in samples from humans and animal autoimmune models[2,3], as well as antibodies generated by vaccination[4], to detect intracellular signaling states[5] and perform multiplex characterization of soluble and cell-surface analytes[6]. Other groups have described array-based approaches that have led to discoveries in cancer[7], neurodegenerative disease[8], aging[9] and allergy[10]. Although these and other innovative array techniques have developed at a rapid pace, technological innovation has not produced adequate tools for the proteome-level assessment of biological and clinical samples on the small and rapid scale that point-of-care medicine demands[11].

Many studies have used an *in silico*, or bioinformatics, approach to characterize pathways or disease states. We hypothesized that creating peptide arrays on a silicon surface ('*on silico*' arrays) could be transformative in the field because an integrated semiconductor circuit could be created beneath each peptide feature, allowing for real-time measurements and computations, neither of which are possible using current fluorescence-based approaches. Here we describe a new, high-density, scalable platform using microprocessor-grade silicon wafers as a support surface (**Supplementary Fig. 1** and **Supplementary Methods**). We used a maskless photolithographic approach to create arrays of overlapping peptides comprising every possible combination of contiguous amino acids within a naturally linear human polypeptide sequence. This synthesis process also permits the incorporation of amino acids modified by the addition of functional groups, for example, lysine that is acetylated or methylated, into a growing peptide sequence, allowing for a subsequent analysis of the interactions with modified and unmodified peptides in parallel on the same microarray. In previous published reports, photolithography has been used in a variety of peptide-conjugation strategies involving both mask-based[12] and maskless[13,14] techniques to generate location-specific peptides on microarray platforms using photolabile or acidlabile Di-*tert*-butyl dicarbonate (*t*-BOC) protective groups; however, these approaches, using glass slides as the synthesis substrate, are difficult and expensive to scale up. In addition, they are limited in the number of unique and overlapping sequences generated, the raw number of discrete peptide addresses and the ability to compare modified and unmodified peptide epitopes in parallel. The use of silicon produces a surface that is highly amenable to fluid-phase detection of peptide-reactive antibodies and other protein-protein interactions. Notably, when using silicon, there is no intrinsic background fluorescence of the surface when imaged in conventional microarray laser scanning systems, and there is no requirement for a preblocking step because of the near absence of nonspecific binding of biological molecules to the surface (data not shown). We successfully leveraged mature semiconductor fabrication technology to produce 68 individual arrays on 6-in silicon wafers. This platform combines advances in two fields, semiconductor

[1]Department of Medicine, Division of Immunology and Rheumatology, Stanford School of Medicine, Stanford, California, USA. [2]Intel Corporation, Santa Clara, California, USA. [3]Department of Biology, Stanford University, Stanford, California, USA. [4]Center for Immunology, University of Minnesota Medical School, Minneapolis, Minnesota, USA. [5]These authors contributed equally to this work. Correspondence should be addressed to J.V.P. (jvprice@stanford.edu) or P.J.U. (pjutz@stanford.edu).

Received 13 June 2011; accepted 2 December 2011; published online 19 August 2012; doi:10.1038/nm.2913

manufacturing and multiplexed biochemical detection, potentially enabling the analysis of multiplex protein-protein interactions in real time. Here we describe the utility of silicon-based peptide arrays, which we have termed Intel arrays, for the high-resolution epitope mapping of diverse commercial monoclonal and polyclonal antibody probes, the characterization of the specific activity of protein lysine methyltransferases and kinases at single–amino-acid precision and the identification of patterns of autoantibody reactivity that correlate significantly with disease severity in a cohort of individuals with systemic lupus erythematosus (SLE).

RESULTS

H2B peptide array design and synthesis

To show the power of the Intel array platform, we fabricated overlapping peptide arrays of a naturally linear region at the N terminus of human histone H2B. H2B is a highly conserved protein that interacts with DNA and other histone proteins that make up the intricate chromatin structures that organize the eukaryotic genome[15]. H2B is a major target for epigenetic regulation that is mediated by post-translational modifications performed by kinases, peptidylarginine deiminases, methyltransferases and acetyltransferases, among others, and manipulation of H2B through the acetylation and methylation of lysine within the linear N-terminal tail of the protein is crucial for the regulation of chromatin homeostasis[16]. Histone epitopes, including the N terminus of H2B, are also clinically important autoantigens in SLE, drug-induced lupus, rheumatoid arthritis and other diseases[2,17,18].

Using a photolithographic process (**Fig. 1a**), we constructed arrays of peptides corresponding to the N-terminal tail of H2B and ranging in length from 1 to 21 amino acids (with the full sequence N_H3-PEPAKSAPAPKKGSKKAVTKA-COOH). The individual arrays were comprised of unmodified peptides, peptides with acetylated lysine at

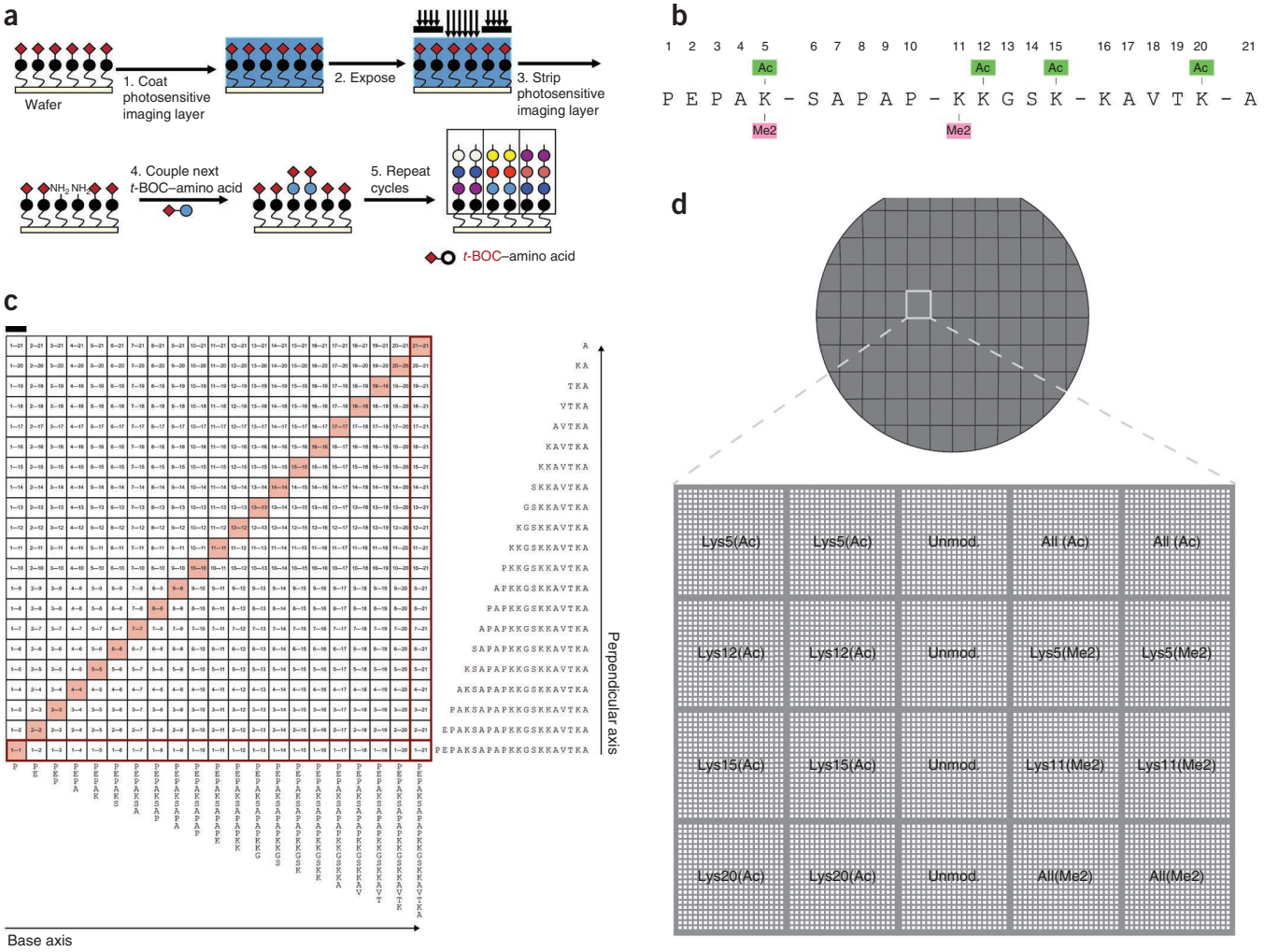

Figure 1 Intel array design and construction. (**a**) Schematic depicting the photolithographic process to synthesize peptide microarrays on silicon wafers (Online Methods). (**b**) 21-mer H2B peptide sequence synthesized on the array with acetylation (Ac) and dimethylation (Me2) sites annotated. (**c**) Layout of features from a representative block on the array. Peptides spanning the 21-mer histone H2B sequence increase by one amino acid to the C terminus along the base axis from left to right and decrease by one amino acid from the N terminus along the perpendicular axis from bottom to top, generating an array of every possible contiguous H2B peptide fragment tiled at single-amino acid increments within the 21-mer sequence. The grid is symmetric along the diagonal axis (highlighted). Peptide sequences for the outermost array features (boxed in red) are shown along the base and perpendicular axes. Scale bar, 50 μm. (**d**) Schematic depicting the diced 6-in silicon wafer containing 68 individual Intel arrays (top). Each array contains 20 square grids organized as depicted in **c** with either an unmodified 21-mer H2B sequence (Unmod.) or a sequence containing acetylated or dimethylated lysine at the indicated positions (bottom).

positions 5, 12, 15 and 20 and peptides with dimethylated lysine at positions 5 and 11 (**Fig. 1b**). Each subarray is a square grid containing every possible peptide fragment within the 21-mer H2B sequence arranged in sequential order (**Fig. 1c**). The H2B array contains 20 square grids that individually contain all possible contiguous H2B peptide lengths, either unmodified or with acetyl and methyl groups incorporated at specific lysine residues within the sequence, totaling 8,820 spatially addressable features (**Fig. 1d**). We routinely assessed the peptide yield, purity and sequence fidelity of the Intel array using on-chip staircase fluorescence assays, off-chip fluorescence HPLC, mass spectrometry and highly sensitive kinase substrate assays and found them to be equivalent to or better than those of the conventional peptide synthesis approaches (**Supplementary Figs. 2–4** and data not shown)[19,20].

Epitope mapping of commercial antibodies using Intel arrays

To determine the ability of Intel arrays to resolve epitopes that are recognized by H2B-reactive antibodies, we probed the arrays with commercial antibodies that have known H2B-binding capacity. Arrays probed with the polyclonal antibody (pAb) 18977 (Abcam), which is directed against the N terminus of H2B, showed a minimum binding epitope of two N-terminal amino acids (**Fig. 2a**). Notably, at higher concentrations, the pAb 18977 also showed moderate binding to peptides containing acetylated Lys5 (Lys5(Ac)) and acetylated Lys12 (Lys12(Ac)), with minimum binding epitopes of three amino acids surrounding acetylated Lys5 (Ala4Lys5(Ac)Ser6) and a 5-mer peptide containing acetylated Lys12 (Lys11Lys12(Ac)Gly13Ser14 Lys15) (data not shown). The monoclonal antibody (mAb) 52988 (Abcam) recognizes the H2B epitope surrounding acetylated Lys20. The Intel arrays showed reactivity at only peptide features containing C-terminal acetylated Lys20, indicating that a minimum peptide length of four amino acids containing acetylated Lys20 is required for the binding of mAb 52988 (**Fig. 2b**). mAb 62335 (Abcam) is directed against an H2B epitope surrounding acetylated Lys15. Intel arrays probed with this antibody revealed reactivity at minimal binding epitopes composed of only two amino acids, Ser14Lys15(Ac)

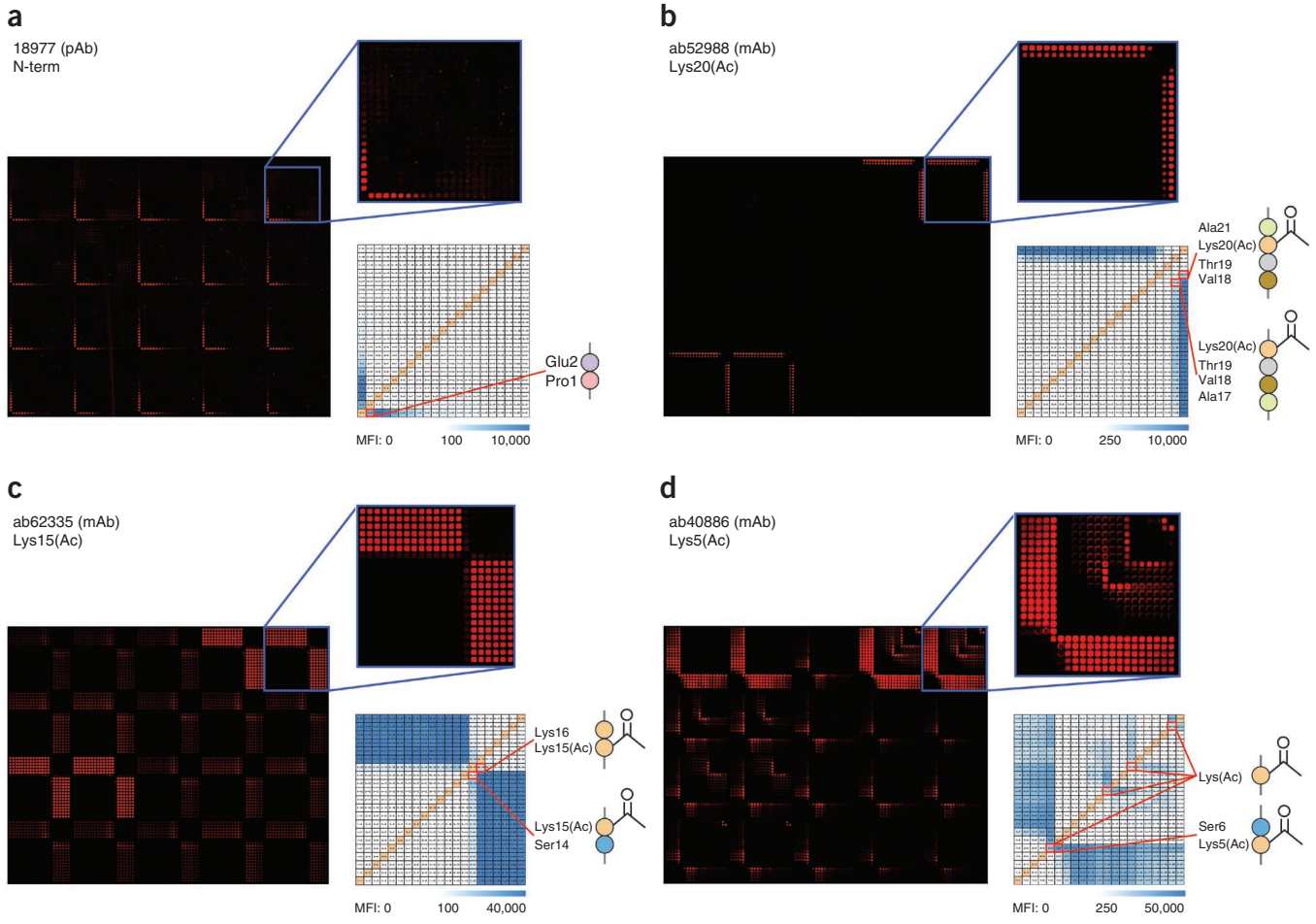

Figure 2 Epitope mapping of polyclonal and monoclonal antibodies using H2B Intel arrays. (**a**) Map with single–amino-acid resolution of the epitope recognized by the H2B-reactive pAb 18977 showing that a minimum of two N-terminal amino acids (Pro1 and Glu2, inset) are required for antibody binding. N-term, N-terminal. (**b**) Epitope map for the mAb 52988, which is directed against residues surrounding acetylated Lys20 (Lys20(Ac)), showing a minimum binding requirement of either Ala17Val18Thr19Lys20(Ac) or Val18Thr19Lys20(Ac)Ala21. (**c**) Epitope map and minimum peptide binding requirements for the mAb 62335, which is directed against residues surrounding Lys15(Ac) of H2B. The minimum binding requirements were determined to be Ser14Lys15(Ac) and Lys15(Ac)Lys16. (**d**) Epitope map for the mAb 40886, which is directed against residues surrounding Lys5(Ac), showing the binding of acetylated lysine (Lys(Ac)), both at position 5 in the context of a peptide of at least 3-mer and also of Lys(Ac) alone or in peptides at positions 12, 15 and 20. For each antibody, the 'All (Ac)' subarray containing acetylated lysine at positions 5, 12, 15 and 20 is enlarged. The grid schematic for each antibody corresponds to reactivity within the enlarged All (Ac) subarray. The color bars indicate the observed median fluorescence intensity (MFI) at each peptide feature.

or Lys15(Ac)Lys16, which contain acetylated Lys15; however, mAb 62335 also showed crossreactivity with both unmodified and dimethylated H2B peptides (**Fig. 2c**). Intel arrays probed with the mAb 40886 (Abcam), which recognizes acetylated Lys5 of H2B, showed reactivity to acetylated Lys5, but we also found binding of the antibody at the acetylated lysines at positions 12, 15 and 20 (**Fig. 2d**). Titrations of the antibodies 52988 and 62335 showed a concentration-dependent decrease in signal on the array, and, compared to indirect ELISA, the array platform showed only slightly decreased sensitivity for antibody 52988 and when using dilutions of antibody 62335 that were at least 2,500× (**Supplementary Fig. 5**). We verified the specific epitopes for each antibody in preclearing experiments using unmodified and acetylated H2B peptides conjugated to sepharose beads (**Supplementary Fig. 6a–e**).

To verify the site-specific methylation of the H2B peptides synthesized on the Intel arrays, we used a rabbit pAb (07-751, Millipore) that is targeted to dimethylated Lys11. We characterized its reactivity not only to a minimum peptide epitope containing dimethylated Lys11 (Lys11(Me2)) (Pro10Lys11(Me2)Lys12) but also to peptides containing dimethylated Lys5 and unmodified peptides (**Fig. 3a**). To assess the nature of the polyclonal reactivity of this antibody, we performed a preclearing experiment using an H2B peptide dimethylated at Lys5.

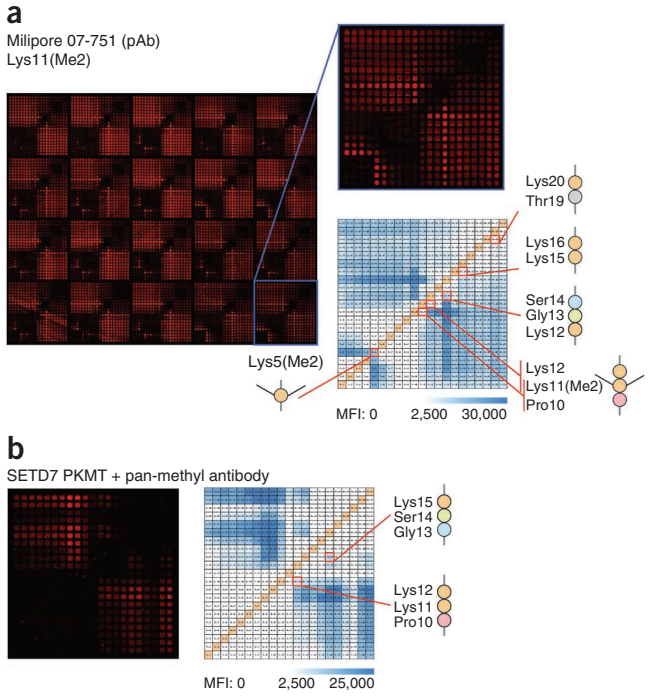

Figure 3 Detection of dimethlyated Intel array peptides and direct monomethylation of lysine-containing Intel array peptides by the PKMT SETD7. (**a**) Epitope map for the pAb directed against dimethylated Lys11 (Lys11(Me2)) (07-751) showing minimum binding requirements of Lys11(Me2) within the 3-mer Pro10Lys11(Me2)Lys12; as well as Lys5(Me2); Lys12Gly13Ser14; Lys15Lys16; and Thr19Lys20. The subarray containing dimethylated lysine at positions 5 and 11, 'All(Me2)', is enlarged. The grid schematic shows the reactivity within the enlarged All(Me2) subarray. (**b**) Scanned image of an Intel array after a PKMT reaction with SETD7 and subsequent detection using a pan-methyl antibody (ab23366). The image and grid schematic show the reactivity within an unmodified subarray. The minimum peptide content required for methylation by SETD7 on the Intel arrays is Pro10Lys11Lys12 or Gly13Ser14Lys15. The color bars indicate the observed median fluorescence intensity (MFI) at each peptide feature.

We found loss of reactivity to peptides containing dimethylated Lys5 but not to peptides containing dimethylated Lys11 or unmodified lysine (**Supplementary Fig. 6f**). This result indicates that within the polyclonal mixture of antibodies constituting the pAb 07-751, there are at least two clones recognizing distinct epitopes of H2B, and further highlights the power of the Intel arrays for deeply characterizing reactivity patterns of mixtures of polyclonal antibodies.

Enzymatic modification of Intel array peptides

Protein lysine methyl transferases (PKMTs) mediate the addition of methyl groups to lysine residues in the N-terminal tail of H2B[16].

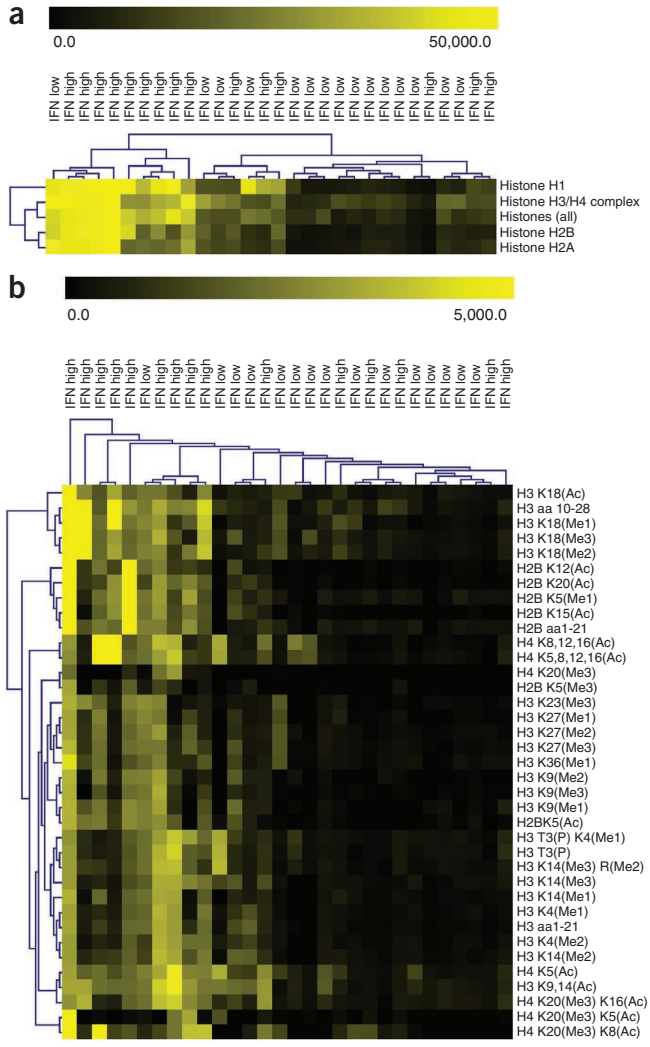

Figure 4 Conventional spotted microarray showing increased reactivity to whole histones and post-translationally modified histone peptides in sera from individuals with IFN-high SLE. (**a**,**b**) Heatmaps showing the hierarchical clustering of peptide features identified using the SAM algorithm as being significantly more reactive (q value < 0.0001) in IFN-high sera. The SAM-identified whole-protein histone antigens (**a**) and peptides (**b**) were statistically more reactive with autoantibodies in the IFN-high sera. Unmodified H2B peptides, as well as H2B peptides with acetylated lysines at position 5, 12, 15 and 20, are among the array features identified by SAM to be significantly associated with disease state in IFN-high SLE (q value < 0.0001). Ac, acetylated; aa, amino acid; Me1, methylated; Me2, dimethylated; Me3, trimethylated; P, phosphorylated. Lysine and threonine are shown with their single-letter amino acid codes (K and T, respectively).

To test whether site-specific methylation can be detected on the Intel arrays, we incubated the arrays with SETD7, a PKMT known to methylate H2B[21]. Incubation with SETD7 resulted in the addition of a single methyl group to several lysine-containing peptides on the Intel Arrays, as detected by probing with a pan-methyl antibody after the PKMT reaction (**Fig. 3b**). Incubation with GST and then with pan-methyl antibody or with pan-methyl antibody alone did not result in the detection of peptide methylation (data not shown). The minimum epitopes required for methylation of the Intel array peptides by SETD7 were Pro10Lys11Lys12 and Gly13Ser14Lys15.

Phosphorylation of H2B is involved in chromatin regulation and is associated with the induction of apoptosis, specifically the phosphorylation of Ser14 (ref. 22). To determine whether specific kinase assays could be performed on the Intel arrays, we synthesized two different microarrays: one with a series of blocks containing sequentially growing peptides spanning a known phosphorylation target peptide (kemptide, LRRASL) of protein kinase A (PKA) (**Supplementary Fig. 7a**) and another with tiled peptides surrounding H2B Ser14 (**Supplementary Fig. 7e**). Intel arrays incubated with PKA showed site-specific phosphorylation of serine residues in both configurations (**Supplementary Fig. 7b–e**). The most optimal orientation for H2B Ser14 phosphorylation seemed to be when Ser14 was flanked by two C-terminal lysine residues; peptides with one lysine C-terminal to Ser14 or in which Ser14 was the most C-terminal amino acid had less phosphorylation (**Supplementary Fig. 7e,f**). This may indicate that there are conformational requirements for the phosphorylation of H2B by PKA.

Autoantibody profiling of SLE sera using Intel arrays

We next assessed the ability of Intel arrays to detect H2B-reactive autoantibodies in human samples. SLE is a heterogeneous disease that is characterized by the development of IgG autoantibodies that are directed against DNA- and RNA-associated proteins of the cell nucleus[23]. Interferon-α (IFN-α) drives autoimmune processes in

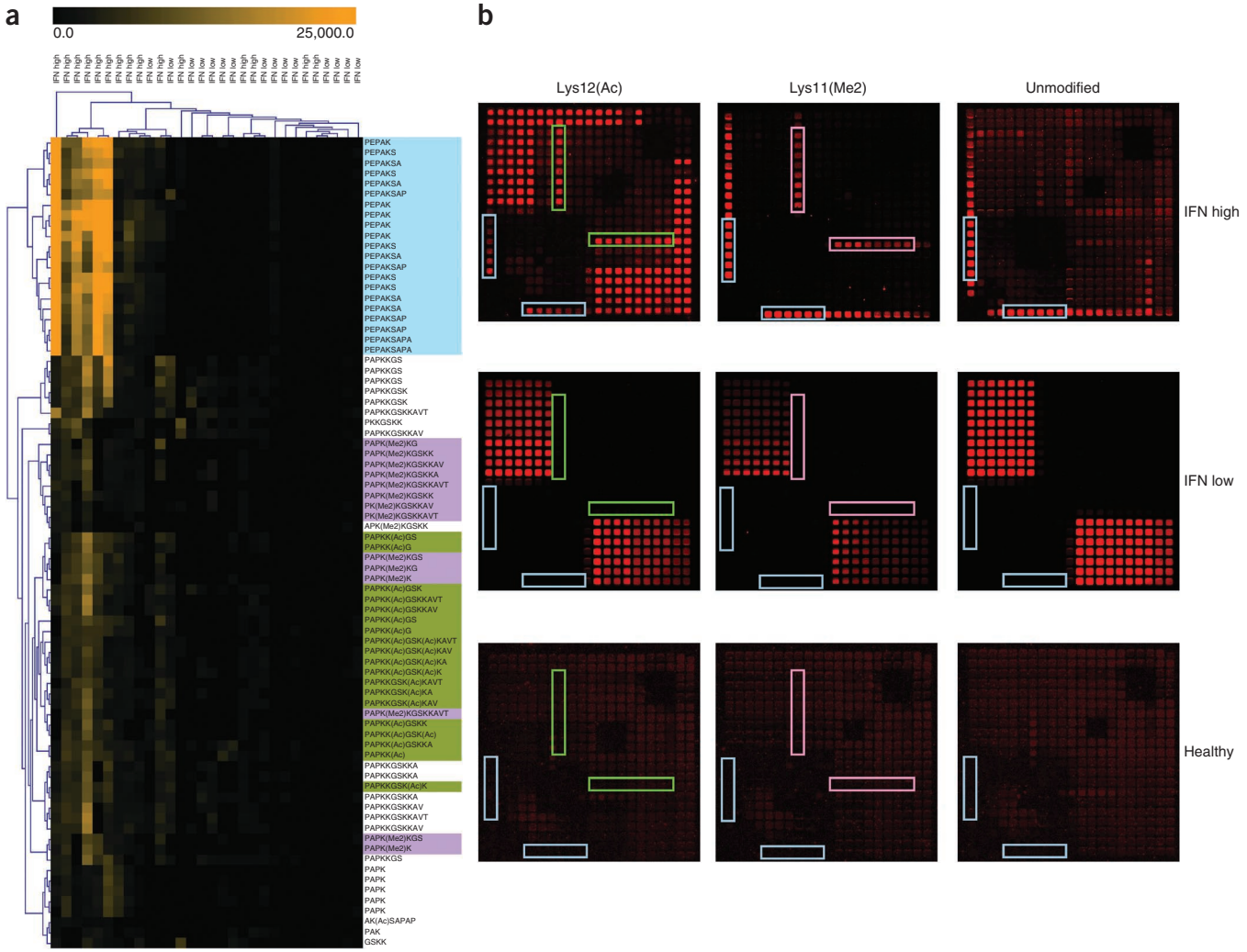

Figure 5 Differential reactivity to histone H2B peptides in a cohort of individuals with SLE. (**a**) Hierarchical clustering of peptide features identified by SAM as being significantly more reactive (q value < 0.0001) in the sera of individuals with IFN-high SLE. Peptides containing the minimum epitope Pro1Glu2Pro3Ala4Lys5 are highlighted in blue; peptides containing acetylated lysine at positions 12 and 15 are highlighted in green; peptides with dimethlyated lysine at position 11 are highlighted in pink. (**b**) Representative images of individual grids from the Intel arrays probed with serum from individuals with IFN-high SLE, individuals with IFN-low SLE and healthy controls. Grids containing H2B peptides with acetylated lysine incorporated at position 12 (left). Grids containing H2B peptides with dimethylated lysine incorporated at position 11 (center). Grids containing unmodified H2B peptides (right). The peptide features in the blue, green and pink boxes correspond to the sequences highlighted in those colors in **a**.

SLE, and the level of IFN-α–driven pathology can be assessed by determining the extent of IFN-α–dependent gene transcription, or the so-called 'interferon signature', with a high interferon signature ('IFN-high') correlating with increased SLE disease severity[24,25]. The presence of serum autoantibodies directed against a variety of nuclear antigens, including histone proteins, is coincident with an overabundance of serum IFN-α in SLE[26]. Furthermore, several reports have described autoantibody reactivity to histone epitopes that are modified post-translationally in mouse models of SLE and human SLE[18,27,28].

Using 30 sera from a cohort of patients with SLE participating in the Autoimmune Biomarkers Collaborative Network (ABCoN) study[29] and profiled for IFN-α–induced gene expression[25], we analyzed IgG reactivity to nucleosomes, individual purified H1, H2A, H2B, a complex of H3 and H4 proteins and peptide fragments with several acetylation and methylation modifications using traditional spotted protein and peptide microarrays[2]. Using Significance Analysis of Microarrays (SAM)[30], we observed that serum IgG autoantibodies from individuals with IFN-high SLE were significantly more reactive to whole-protein histone antigens (q value < 0.0001; **Fig. 4a**), as well as to unmodified full-length H2B peptides and H2B peptides containing acetylated lysine at positions 5, 12, 15 and 20 (q value < 0.0001; **Fig. 4b**).

We tested whether Intel arrays could replicate our findings that serum from individuals with IFN-high SLE is more reactive to unmodified H2B peptides and H2B peptides with modified functional groups than serum from individuals with IFN-low SLE, as well as whether high-resolution mapping could define immunogenic regions of H2B in IFN-α–driven SLE. The SAM algorithm identified several classes of peptides on the Intel arrays that were significantly more reactive to IgG from sera of individuals with IFN-high SLE (q value < 0.0001; **Fig. 5a**). These included an unmodified region near the N terminus of the peptide with a minimum amino acid sequence of Pro1–Lys5 (Pro1Glu2Pro3Ala4Lys5), several peptides containing acetylated Lys12 and acetylated Lys15 and peptides containing dimethylated Lys11 (**Fig. 5a**,**b**). Reactivity to peptides containing Pro1–Lys5, acetylated Lys12, acetylated Lys15 or dimethylated Lys11 was largely absent in sera from individuals with IFN-low SLE and healthy controls (**Fig. 5b**). We performed an ELISA validation of the Intel array reactivity using full-length and truncated H2B peptides and confirmed that serum from individuals with IFN-high SLE was significantly more reactive to N-terminal H2B and to acetylated Lys12 and acetylated Lys15 of H2B (P < 0.05; **Supplementary Fig. 8**). These data suggest that N-terminal reactivity to the minimum sequence Pro1–Lys5, as well as reactivity to epitopes surrounding the indicated acetylated and dimethylated lysine residues, may be important for breaking tolerance to H2B and furthering autoantibody pathogenesis in IFN-α–driven SLE.

DISCUSSION

Intel arrays constitute a considerable advance in proteomic analysis as the first highly multiplex array platform with single–amino-acid resolution that has utility in a variety of proteomic studies, including epitope mapping and the characterization of diverse protein-protein interactions. We showed the utility of the Intel arrays in epitope mapping of commercial antibodies directed against H2B. The ability of the Intel arrays to resolve the reactivity of commercial antibodies to peptides as small as two amino acids speaks to the high degree of sensitivity and specificity of the platform and shows its potential for investigating basic immunological issues, such as the precise epitopes that are recognized by antibodies. A high-resolution epitope mapping platform has application far beyond the characterization of chromatin-binding antibodies. Within the last decade, there has been great advancement of new monoclonal antibodies and other protein engineering technologies that are geared toward the development of disease therapeutics[31]. As the field of antibody and protein engineering evolves, it will be necessary to develop rapid, multiplex, cost-effective testing platforms to determine precise target epitopes, obtain information about interaction kinetics and determine whether there is crossreactivity that may impede or enhance the activity of engineered molecules.

We showed the ability of the Intel arrays to detect the sequence-specific activity of the PKMT SETD7 and PKA. These proof-of-concept experiments demonstrate the power of Intel arrays for the discovery of new targets of these and other protein-modification enzymes. We have recently shown that a combination of methylation and phosphorylation regulates lymphocyte inflammatory responses through modifications of the NF-κB protein RelA by the PKMT SETD6 and protein kinase C, ζ (PKC-ζ)[32]. Peptide arrays have been instrumental in the discovery of these and other methylation targets of PKMTs[21], suggesting that Intel arrays will be useful in this field. Kinases and PKMTs are the targets of specific inhibitors, many of which have entered clinical trials for the treatment of cancer and other diseases[33]. Given the ability of Intel arrays to resolve the specific activity of kinases and PKMT enzymes in parallel, we believe that this platform is well suited for inhibitor screening.

We also showed the utility of Intel arrays in defining epitopes within unmodified and post-translationally modified H2B that are associated with IFN-α–driven SLE. The identification of specific epitopes within this important antigen may help better define IFN-α–driven autoantibody pathogenesis in SLE. As inhibitors of IFN-α and its receptor, IFNAR, have entered phase 2 clinical trials in SLE, these arrays may be useful in determining relevant clinical outcomes. Our results corroborate reports showing that autoantibodies targeting post-translational modifications on histone proteins, notably acetylated and methylated epitopes, are associated with SLE pathogenesis[18,27,28]. They also underscore the idea that high-resolution mapping on the Intel array platform has great potential for identifying immunogenic regions that are relevant to the pathogenesis of SLE in a rapid and reliable way. Although peptide-based approaches have not been developed sufficiently to replace the gold-standard antibody detection tests performed in most clinics, several peptide platforms have been used in the routine diagnosis of autoimmune diseases, including celiac disease[34] and rheumatoid arthritis[35,36], and have been used to guide a phase 2 vaccine trial in multiple sclerosis[37]. Accordingly, the Intel array platform holds great promise in expanding the use of peptide-based diagnostic technology for the detection of relevant antibody reactivity in the clinical setting.

One potential limitation of peptide arrays is their reliance on linear peptide sequences, which precludes an assessment of conformational protein epitopes. This limitation in characterizing protein-protein interactions will diminish as technological advances improve the diversity of protein conformations 'in miniature'. Combining Intel array technology with emerging advances in the synthesis of peptide mimetics could directly address this limitation[38].

Magnetic nanosensors are currently being developed to couple high-resolution Intel peptide arrays with underlying, *in silico* technology, facilitating real-time detection of the kinetics of antibody-peptide interactions. Furthermore, we anticipate the rapid integration of the Intel peptide array platform into existing magnetic nanosensor

point-of-care technology[39]. The combination of these technologies will yield a revolutionary tool for personalized, point-of-care proteomics and allow for reactions on submicron array features to be detected in real time.

METHODS

Methods and any associated references are available in the online version of the paper.

Accession codes. All microarray data are deposited in the Gene Expression Omnibus with accession codes GSE34034 (for data in **Figs. 2** and **3**) and GSE34070 (for data in **Figs. 4** and **5**).

Note: Supplementary information is available in the online version of the paper.

ACKNOWLEDGMENTS

We thank H. Lee, J. Zhu and the other members of the peptide array team at Biomedical Life Science at Digital Health Intel for development of the early peptide array process and G. Credo for help with the Online Methods section of the manuscript. We thank D. Hall, K.C. Garcia, S. Sidhu, J. Haddon, J. Jarrell and other members of our laboratories for helpful discussion. J.V.P. was funded by a US National Science Foundation Graduate Research Fellowship (NSF GRFP) and is supported by the Stanford Genome Training Program (SGTP; US National Institutes of Health (NIH), US National Human Genome Research Institute). D.L. is supported by the European Molecular Biology Organization, the Human Frontier Science Program and the Machiah Foundation. O.G. is a recipient of an Ellison Senior Scholar Award and is funded by a grant from the NIH (R01 GM079641). P.J.U. is the recipient of a Donald E. and Delia B. Baxter Foundation Career Development Award and is supported by National Heart, Lung, and Blood Institute (NHLBI) Proteomics contract HHSN288201000034C, Proteomics of Inflammatory Immunity and Pulmonary Arterial Hypertension; grants from the NIH (5 U19-AI082719, 5 U19-AI050864, 5 U19-AI056363, 1 U19 AI090019 and 4 U19 AI090019); Canadian Institutes of Health Research (2 OR-92141); Alliance for Lupus Research (grant number 21858); a gift from the Ben May Trust and a gift from the Floren Family Trust. The research leading to these results has received funding from the European Union Seventh Framework Programme (FP7/2007-2013) under grant agreement number 261382. C.L.L. is a recipient of an NIH National Research Service Award Fellowship (5 F32 AI-080086-02).

AUTHOR CONTRIBUTIONS

J.V.P. conducted antibody-binding experiments and ELISA, analyzed the data, made the figures and wrote the manuscript. S.T. performed antibody-binding experiments and contributed to data analysis and figure production. G.X. and J.Y. designed and fabricated Intel arrays. D.L. and O.G. contributed the methylation assay. E.C.B. characterized the IFN signature and provided ABCoN patient samples. M.V. supervised the development team at Intel and edited the manuscript. P.J.U. and C.L.L. supervised the project and edited the manuscript.

COMPETING FINANCIAL INTERESTS

The authors declare competing financial interests: details are available in the online version of the paper.

Published online at http://www.nature.com/doifinder/10.1038/nm.2913.
Reprints and permissions information is available online at http://www.nature.com/reprints/index.html.

1. Cortese, D.A. A vision of individualized medicine in the context of global health. *Clin. Pharmacol. Ther.* **82**, 491–493 (2007).
2. Robinson, W.H. *et al.* Autoantigen microarrays for multiplex characterization of autoantibody responses. *Nat. Med.* **8**, 295–301 (2002).
3. Robinson, W.H. *et al.* Protein microarrays guide tolerizing DNA vaccine treatment of autoimmune encephalomyelitis. *Nat. Biotechnol.* **21**, 1033–1039 (2003).
4. Neuman de Vegvar, H.E. *et al.* Microarray profiling of antibody responses against simian-human immunodeficiency virus: postchallenge convergence of reactivities independent of host histocompatibility type and vaccine regimen. *J. Virol.* **77**, 11125–11138 (2003).
5. Chan, S.M., Ermann, J., Su, L., Fathman, C.G. & Utz, P.J. Protein microarrays for multiplex analysis of signal transduction pathways. *Nat. Med.* **10**, 1390–1396 (2004).
6. Kattah, M.G., Coller, J., Cheung, R.K., Oshidary, N. & Utz, P.J. HIT: a versatile proteomics platform for multianalyte phenotyping of cytokines, intracellular proteins and surface molecules. *Nat. Med.* **14**, 1284–1289 (2008).
7. Haab, B.B. Antibody arrays in cancer research. *Mol. Cell. Proteomics* **4**, 377–383 (2005).
8. Ray, S. *et al.* Classification and prediction of clinical Alzheimer's diagnosis based on plasma signaling proteins. *Nat. Med.* **13**, 1359–1362 (2007).
9. Britschgi, M. *et al.* Neuroprotective natural antibodies to assemblies of amyloidogenic peptides decrease with normal aging and advancing Alzheimer's disease. *Proc. Natl. Acad. Sci. USA* **106**, 12145–12150 (2009).
10. Vigh-Conrad, K.A., Conrad, D.F. & Preuss, D. A protein allergen microarray detects specific IgE to pollen surface, cytoplasmic, and commercial allergen extracts. *PLoS ONE* **5**, e10174 (2010).
11. Bailey, R.C. Grand challenge commentary: informative diagnostics for personalized medicine. *Nat. Chem. Biol.* **6**, 857–859 (2010).
12. Fodor, S.P. *et al.* Light-directed, spatially addressable parallel chemical synthesis. *Science* **251**, 767–773 (1991).
13. Gao, X., Zhou, X. & Gulari, E. Light directed massively parallel on-chip synthesis of peptide arrays with t-Boc chemistry. *Proteomics* **3**, 2135–2141 (2003).
14. Shin, D.S. *et al.* Automated maskless photolithography system for peptide microarray synthesis on a chip. *J. Comb. Chem.* **12**, 463–471 (2010).
15. Khorasanizadeh, S. The nucleosome: from genomic organization to genomic regulation. *Cell* **116**, 259–272 (2004).
16. Kouzarides, T. Chromatin modifications and their function. *Cell* **128**, 693–705 (2007).
17. Monestier, M., Decker, P., Briand, J.P., Gabriel, J.L. & Muller, S. Molecular and structural properties of three autoimmune IgG monoclonal antibodies to histone H2B. *J. Biol. Chem.* **275**, 13558–13563 (2000).
18. van Bavel, C.C. *et al.* Apoptosis-associated acetylation on histone H2B is an epitope for lupus autoantibodies. *Mol. Immunol.* **47**, 511–516 (2009).
19. Barone, A.D. *et al.* Photolithographic synthesis of high-density oligonucleotide probe arrays. *Nucleosides Nucleotides Nucleic Acids* **20**, 525–531 (2001).
20. Lee, M.S. & Kerns, E.H. LC/MS applications in drug development. *Mass Spectrom. Rev.* **18**, 187–279 (1999).
21. Dhayalan, A., Kudithipudi, S., Rathert, P. & Jeltsch, A. Specificity analysis–based identification of new methylation targets of the SET7/9 protein lysine methyltransferase. *Chem. Biol.* **18**, 111–120 (2011).
22. Cheung, W.L. *et al.* Apoptotic phosphorylation of histone H2B is mediated by mammalian sterile twenty kinase. *Cell* **113**, 507–517 (2003).
23. von Mühlen, C.A. & Tan, E.M. Autoantibodies in the diagnosis of systemic rheumatic diseases. *Semin. Arthritis Rheum.* **24**, 323–358 (1995).
24. Baechler, E.C. *et al.* Interferon-inducible gene expression signature in peripheral blood cells of patients with severe lupus. *Proc. Natl. Acad. Sci. USA* **100**, 2610–2615 (2003).
25. Bauer, J.W. *et al.* Elevated serum levels of interferon-regulated chemokines are biomarkers for active human systemic lupus erythematosus. *PLoS Med.* **3**, e491 (2006).
26. Obermoser, G. & Pascual, V. The interferon-α signature of systemic lupus erythematosus. *Lupus* **19**, 1012–1019 (2010).
27. Dieker, J.W. *et al.* Apoptosis-induced acetylation of histones is pathogenic in systemic lupus erythematosus. *Arthritis Rheum.* **56**, 1921–1933 (2007).
28. van Bavel, C.C. *et al.* Apoptosis-induced histone H3 methylation is targeted by autoantibodies in systemic lupus erythematosus. *Ann. Rheum. Dis.* **70**, 201–207 (2011).
29. Petri, M. Hopkins Lupus Cohort. 1999 update. *Rheum. Dis. Clin. North Am.* **26**, 199–213, v (2000).
30. Tusher, V.G., Tibshirani, R. & Chu, G. Significance analysis of microarrays applied to the ionizing radiation response. *Proc. Natl. Acad. Sci. USA* **98**, 5116–5121 (2001).
31. Baker, M. Upping the ante on antibodies. *Nat. Biotechnol.* **23**, 1065–1072 (2005).
32. Levy, D. *et al.* Lysine methylation of the NF-κB subunit RelA by SETD6 couples activity of the histone methyltransferase GLP at chromatin to tonic repression of NF-κB signaling. *Nat. Immunol.* **12**, 29–36 (2011).
33. Yoo, C.B. & Jones, P.A. Epigenetic therapy of cancer: past, present and future. *Nat. Rev. Drug Discov.* **5**, 37–50 (2006).
34. Volta, U. *et al.* Deamidated gliadin peptide antibodies as a routine test for celiac disease: a prospective analysis. *J. Clin. Gastroenterol.* **44**, 186–190 (2010).
35. Lee, D.M. & Schur, P.H. Clinical utility of the anti-CCP assay in patients with rheumatic diseases. *Ann. Rheum. Dis.* **62**, 870–874 (2003).
36. Hoffman, I.E. *et al.* Diagnostic performance and predictive value of rheumatoid factor, anti-citrullinated peptide antibodies, and the HLA shared epitope for diagnosis of rheumatoid arthritis. *Clin. Chem.* **51**, 261–263 (2005).
37. Garren, H. *et al.* Phase 2 trial of a DNA vaccine encoding myelin basic protein for multiple sclerosis. *Ann. Neurol.* **63**, 611–620 (2008).
38. Liskamp, R.M.J., Rijkers, D.T.S., Kruijtzer, J.A.W. & Kemmink, J. Peptides and proteins as a continuing exciting source of inspiration for peptidomimetics. *ChemBioChem* **12**, 1626–1653 (2011).
39. Gaster, R.S., Hall, D.A. & Wang, S.X. nanoLAB: an ultraportable, handheld diagnostic laboratory for global health. *Lab Chip* **11**, 950–956 (2011).

ONLINE METHODS

Wafer derivatization and linker attachment. We derivatized blank 6-in silicon wafers (Silicon Valley Microelectronics, Santa Clara, CA) by thermal oxidation and then performed salination by immersion in a 0.5% (v/v) mixture of 3-aminopropyltriethoxysilane (Sigma-Aldrich, St. Louis, MO) in 95% ethyl alcohol (EtOH, Sigma) for 30 min at room temperature. We then cured the wafers at 100 °C for 1 h under ultrapure and ultradry N_2 (Airgas, Sacramento, CA) to crosslink the silane groups to each other and to the silicon surface. After salination, we added a polyethylene glycol $(PEG)_6$ linker to the wafer surface to facilitate the addition of custom peptides.

Array patterning by photolithography and amino acid coupling. For wafer-scale array patterning, we used a spin coater (Brewer Science, Rolla, MO) to apply a photosensitive imaging solution containing a photoacid generator and a sensitizer in propylene glycol methyl ether acetate (PGMEA, Sigma). In a class-10,000 clean room, we mounted the wafers on a computer-controlled X-Y stage (Newport Corporation, Irvine, CA) and patterned the array features by exposing selected areas of the wafer to ultraviolet (UV) light though a virtual mask with a digital exposure tool modified from a digital light processing (DLP) device (Texas Instruments, Dallas, TX). At each coupling step, we treated the UV-exposed wafers with coupling solution (*t*-BOC amino acid of interest (Novabiochem, San Diego, CA), hydroxybenzotriazole (HOBt, CPC Scientific, Sunnyvale, CA) and *N,N′*-diisopropylcarbodiimide (DIC, CPC Scientific) dissolved in *N*-Methyl-2-pyrrolidone (NMP, Sigma) with a final concentration of 0.1 M each) for 30 min at room temperature. After a brief rinse in *N,N*-dimethylformamide (DMF, Sigma), we transferred the wafers into capping solution (5% Ac_2O in DMF). We then washed the wafers extensively in DMF and 2-propanol (IPA, Sigma) in preparation for the subsequent photolithography step.

Antibody-binding assays. We equilibrated the deprotected arrays by washing three times in PBS (Bio-Rad, Hercules, CA) and 0.1% Tween-20 (Sigma) (PBST), once in PBS and then once in distilled H_20. We diluted the commercial antibodies or serum from patients in peptide binding buffer (PBB) (50 mM Tris (Mallinckrodt Baker, Phillipsburg, NJ), pH 7.5, 150 mM NaCl (Mallinckrodt AR, Phillipsburg, NJ), 0.05% NP-40 (Sigma) and 2.5% fetal calf serum (FCS, Omega Scientific, Tarzana, CA)) and applied the samples to arrays in 12-well tissue culture plates (Fisher Scientific, Pittsburg, PA) overnight at 4 °C on a rocking platform. We diluted all primary antibodies ((ab18977, ab52988, ab62335, ab40886, Abcam) (07-751, Millipore)) 1:1,000 from the original stocks as received from the vendors. After three washes in PBST, we applied secondary goat mouse IgG-specific Cy5-conjugated antibody (115-175-146, Jackson Immunoresearch, West Grove, PA), goat rabbit IgG-specific Alexa Fluor 647-conjugated antibody (A-31573, Invitrogen, Carlsbad, CA) or goat human IgG-specific Cy5-conjugated antibody (109-495-129, Jackson) diluted to 0.375 μg ml^{-1} in PBST and 20% FCS for 45 min at room temperature on a rocking platform. We then washed the arrays three times for 5 min each in PBST and briefly rinsed them in PBS and distilled H_20 before drying them in microscope slide racks centrifuged at 300 *g* for 5 min at room temperature. We immediately scanned and processed the arrays using an Axon digital scanning system and performed analyses using Genepix Pro 6.1 software (Molecular Devices, Sunnyvale, CA).

Methylation assay. We incubated arrays in a 12-well plate overnight on a rocking platform at 30 °C in a reaction mixture containing 60 μg SETD7 or GST purified proteins and 0.1 mM *S*-adenosylmethionine (AdoMet, Sigma) in a methylation buffer containing 50 mM Tris-HCl (pH 8.0), 10% glycerol, 20 mM KCl, 5 mM $MgCl_2$ and 1 mM phenylmethanesulfonyl fluoride (Roche Pharmaceuticals, San Francisco, CA) in a total reaction volume of 500 μl. After the methylation reaction, we washed the arrays three times with PBST and then washed them three times in PBST and 20% FCS. We then visualized the array peptide monomethylation using a rabbit polyclonal pan-methyl antibody (ab23366, Abcam, Cambridge, MA) diluted to 0.25 μg ml^{-1} in PBST and 20% FCS.

Preclearing and peptide competition assay. For the preclearing experiments, we incubated streptavidin-sepharose beads (GE Healthcare, Piscataway, NJ) with 0.2 mg ml^{-1} unmodified biotinylated histone peptide H2B 1–21, H2B 1–21 acetylated at Lys5, Lys12, Lys15 and Lys20 or H2B 1–21 containing dimethylated Lys5 (W.M. Keck Foundation, Yale University) for 30 min at room temperature, washed them twice in PBS and 10% FCS and then incubated the peptide-bound beads with commercial antibodies ((ab18977, ab52988, ab62335, ab40886, Abcam) (07-751, Millipore)) diluted 1:1,000 in PBB and 2.5% FCS for 20 min at room temperature. We then centrifuged the bead and antibody mixture at 850 *g* for 1 min to pellet the bead complexes. We repeated this procedure five times before incubation of the precleared sample on arrays.

Sources of human samples and storage. We used serum samples from patients with SLE collected as part of the ABCoN[29] maintained at −80 °C. Clinical information and research protocols for study enrollment, sample collection and processing are available as previously reported[25]. Approval for use of the ABCoN samples was granted by the University of Minnesota Institutional Review Board, 0110M09982, last approval date 10/13/2011.

Additional methods. Detailed methodology is described in the **Supplementary Methods**.